

## Research Article

# Hill Problem Analytical Theory to the Order Four: Application to the Computation of Frozen Orbits around Planetary Satellites

**Martin Lara<sup>1</sup> and Jesús F. Palacián<sup>2</sup>**

<sup>1</sup> *Celestial Mechanics Division, Real Observatorio de la Armada, 11110 San Fernando, Spain*

<sup>2</sup> *Departamento de Ingeniería Matemática e Informática, Universidad Pública de Navarra, 31006 Pamplona, Spain*

Correspondence should be addressed to Martin Lara, mlara@roa.es

Received 7 June 2009; Accepted 24 August 2009

Recommended by Silvia Maria Giuliatti Winter

Frozen orbits of the Hill problem are determined in the double-averaged problem, where short and long-period terms are removed by means of Lie transforms. Due to the perturbation method we use, the initial conditions of corresponding quasi-periodic solutions in the nonaveraged problem are computed straightforwardly. Moreover, the method provides the explicit equations of the transformation that connects the averaged and nonaveraged models. A fourth-order analytical theory is necessary for the accurate computation of quasi-periodic frozen orbits.

Copyright © 2009 M. Lara and J. F. Palacián. This is an open access article distributed under the Creative Commons Attribution License, which permits unrestricted use, distribution, and reproduction in any medium, provided the original work is properly cited.

## 1. Introduction

Besides its original application to the motion of the Moon [1], the Hill problem provides a good approximation to the real dynamics of a variety of systems, encompassing the motion of comets, natural and artificial satellites, distant moons of asteroids, or dynamical astronomy applications [2–4]. Specifically, the Hill model and its variations [5–9] are useful for describing the motion about planetary satellites. In addition, the Hill problem is an invariant model that does not depend on any parameter, thus, giving broad generality to the results, whose application to different systems becomes a simple matter of scaling. Note that Hill's case of orbits close to the smaller primary is a simplification of the restricted three-body problem, which in turn is a simplification of real models.

A classical result shows that low eccentricity orbits around a primary body are unstable for moderate and high inclinations due to third-body perturbations [10]. Almost circular orbits close to the central body remain with low eccentricity in the long-term only when the mutual inclination with the perturbing body is less than the critical inclination of the third-body perturbations  $I = 39.2^\circ$  (see [11] and references therein). Because of their

low eccentricity, high inclination orbits are precisely the candidate orbits for science missions around natural satellites. Therefore, a good understanding of the unstable dynamics of the Hill problem is required.

The study of the long-term dynamics is usually done in the double-averaged problem. After removing the short- and long-period terms, and truncating higher-order terms, the problem is reduced to one degree of freedom in the eccentricity and the argument of the periapsis. As the double-averaged problem is integrable and the corresponding phase space is a compact manifold, the solutions are closed curves and equilibria. The latter are orbits that, on average, have almost constant eccentricity and fixed argument of the periapsis, and are known as frozen orbits.

To each trajectory of the double-averaged problem it corresponds a torus of quasiperiodic solutions in the nonaveraged problem. The accurate computation of initial conditions on the torus requires the recovery of the short- and long-period effects that were eliminated in the averaging. This is normally done by trial and error, making iterative corrections on the orbital elements, although other procedures can be applied [12].

Our analytical theory is computed with Deprit's perturbation technique [13]. The procedure is systematic and has the advantage of providing the explicit transformation equations that connect the averaged analysis with proper initial conditions of the nonaveraged problem. A second-order truncation of the Hamiltonian shows that there are no degenerate equilibria and, therefore, it is sufficient to give the qualitative description of the reduced system. However, the second-order truncation introduces a symmetry between the direct and retrograde orbits that is not part of the original problem, and a third-order truncation is required to reveal the nonsymmetries of the problem.

While, in general, the third-order theory provides good results in the computation of quasiperiodic, frozen orbits, its solutions are slightly affected by long-period oscillations. This fact may adversely affect the long-term evolution of the frozen orbits and it becomes apparent in the computation of science orbits about planetary satellites, a case in which small perturbations are enough for the unstable dynamics to defrost the argument of the periapsis. Then, the orbit immediately migrates along the unstable manifold with an exponential increase in the eccentricity.

We find that a higher-order truncation is desirable if one wants to use the analytical theory for computing accurate initial conditions of frozen orbits. The computation of the fourth-order truncation removes almost all adverse effects from the quasiperiodic solutions, and shows a high degree of agreement between the averaged and nonaveraged models even in the case of unstable orbits.

Whereas the third-body perturbation is the most important effect in destabilizing science orbits around planetary satellites, the impact of the nonsphericity of the central body may be taken into account. The previous research including both effects has been limited up to third-order theories (see [14] and references therein), but from the conclusions of this paper it may worth to develop a higher-order theory including the inhomogeneities of the satellite's gravitational potential.

## 2. Double-Averaged Hill Problem to the Fourth-Order

The equations of motion of the Hill problem are derived from the Hamiltonian

$$\mathcal{H} = \left(\frac{1}{2}\right) (\mathbf{X} \cdot \mathbf{X}) - \boldsymbol{\omega} \cdot (\mathbf{x} \times \mathbf{X}) + W(\mathbf{x}), \quad W = \left(\frac{\omega^2}{2}\right) (r^2 - 3x^2) - \frac{\mu}{r}, \quad (2.1)$$

where, in the standard coordinate system of Hill's model,  $\mathbf{x} = (x, y, z)$  is the position vector,  $\mathbf{X} = (X, Y, Z)$  is the vector of conjugate momenta,  $r = \|\mathbf{x}\|$ , and both the rotation rate of the system  $\omega = \|\boldsymbol{\omega}\|$  and the gravitational parameter  $\mu$  of the primary are set to 1 in appropriate units.

The problem is of three degrees of freedom, yet admitting the Jacobi constant  $\mathcal{H} = -C/2$ . Despite its nonintegrability, approximate solutions that explain the long-term dynamics can be found by perturbation methods. Close to the central body the Hill problem can be written as the perturbed two-body problem

$$\mathcal{H} = \left(\frac{1}{2}\right)(X^2 + Y^2 + Z^2) - \left(\frac{1}{r}\right) - \epsilon (x Y - y X) + \left(\frac{\epsilon^2}{2}\right)(r^2 - 3x^2), \quad (2.2)$$

where the first three terms of Hamiltonian (2.2) correspond to the Keplerian motion in the rotating frame and  $\epsilon$  is a formal parameter introduced to manifest the importance of each effect. Thus, the Coriolis term is a first order effect and the third-body perturbation appears at the second-order.

To apply perturbation theory, we formulate the problem in Delaunay variables  $(\ell, g, h, L, G, H)$ , where  $\ell$  is the mean anomaly,  $g$  is the argument of the periapsis,  $h$  the argument of the node in the rotating frame,  $L = \sqrt{\mu a}$  is the Delaunay action,  $G = L \sqrt{1 - e^2}$  is the modulus of the angular momentum vector,  $H = G \cos I$  is its polar component, and  $a, e, I$ , are usual orbital elements: semimajor axis, eccentricity, and inclination.

Our theory is based on the use of Lie transforms as described by Deprit [13, 15]. It has the advantage of connecting the averaged and original problems through explicit transformation equations. After removing the short- and long-period terms we get the transformed Hamiltonian

$$\mathcal{K} = K_{0,0} + \epsilon K_{0,1} + \left(\frac{\epsilon^2}{2}\right) K_{0,2} + \left(\frac{\epsilon^3}{6}\right) K_{0,3} + \left(\frac{\epsilon^4}{24}\right) K_{0,4}, \quad (2.3)$$

where  $\epsilon = L^3$ ,

$$K_{0,0} = -\frac{1}{(2L^2)},$$

$$K_{0,1} = K_{0,0} 2\sigma,$$

$$K_{0,2} = K_{0,0} \left(\frac{1}{4}\right) \left[ (2 + 3e^2) (2 - 3s^2) + 15e^2 s^2 \cos 2g \right],$$

$$K_{0,3} = K_{0,0} \left(\frac{27}{32}\right) \sigma \left[ 2s^2 + (50 - 17s^2)e^2 + 15e^2 s^2 \cos 2g \right],$$

$$\begin{aligned} K_{0,4} = K_{0,0} \left(-\frac{3}{512}\right) & \left\{ 3285s^4 e^4 \cos 4g - 12s^2 \left[ 3996 - 2940s^2 - (4582 - 4035s^2) e^2 \right] e^2 \cos 2g \right. \\ & + 8(784 - 708s^2 - 9s^4) - 144(926 - 941s^2 + 244s^4) e^2 \\ & \left. + 9(10728 - 15208s^2 + 5007s^4) e^4 \right\}, \end{aligned} \quad (2.4)$$

and  $\sigma = H/L = c\eta$ ,  $\eta = \sqrt{1 - e^2}$  is the eccentricity function, and we use the abbreviations  $s \equiv \sin I$ ,  $c \equiv \cos I$ . Details on the perturbation method and expressions to compute the transformation equations of the averaging are given in the appendix.

The double-averaged Hamiltonian (2.3) depends neither on the mean anomaly nor on the argument of the node. Therefore, the corresponding conjugate momenta,  $L$  and  $H$ , are integrals of the reduced problem and the Hamiltonian (2.3) represents a one degree of freedom problem in  $g$  and  $G$ . The equations of motion are computed from Hamilton equations  $dg/dt = \partial\mathcal{K}/\partial G$ ,  $dG/dt = -\partial\mathcal{K}/\partial g$ ,

$$\begin{aligned} \frac{dg}{dt} = & \frac{6}{G} [5c^2 - \eta^2 - 5(c^2 - \eta^2) \cos 2g] + \frac{27\varepsilon\sigma}{4G} [5c^2 + 11\eta^2 - 5(c^2 - \eta^2) \cos 2g] \\ & + \frac{3\varepsilon^2}{128G} \left\{ 2113c^2 - 3285c^4 + (3915 + 9165c^4)\eta^2 + (1581 + 7791c^2)\eta^4 \right. \\ & \quad - 4[802c^2 - 1095c^4 + (19 + 2565c^4)\eta^2 - (547 + 1744c^2)\eta^4] \cos 2g \\ & \quad \left. + 1095e^2s^2(c^2 - \eta^2) \cos 4g \right\}, \end{aligned} \quad (2.5)$$

$$\begin{aligned} \frac{dG}{dt} = & -\frac{3}{4}e^2s^2 \left\{ 5(8 + 9\varepsilon\sigma) \sin 2g \right. \\ & \left. + \frac{\varepsilon^2}{32} \left( 2[509 - 1095c^2 + (547 + 4035c^2)\eta^2] \sin 2g - 1095e^2s^2 \sin 4g \right) \right\}. \end{aligned}$$

Once  $g$  and  $G$  are integrated for given initial conditions, the secular variations of  $\ell$  and  $h$  are computed from simple quadratures derived from Hamilton equations  $dh/dt = \partial\mathcal{K}/\partial H$ ,  $d\ell/dt = \partial\mathcal{K}/\partial L$ ,

$$h = h_0 + \int \frac{\partial}{\partial H} \mathcal{K}(g(t), G(t); H, L) dt, \quad \ell = \ell_0 + \int \frac{\partial}{\partial L} \mathcal{K}(g(t), G(t); H, L) dt. \quad (2.6)$$

### 3. Qualitative Dynamics

The flow can be integrated from the differential equations mentioned previously, (2.5). However, since the system defined by (2.5) is integrable, the flow is made of closed curves and equilibria, and it can be represented by contour plots of Hamiltonian (2.3). Thus, for given values of the dynamical parameters  $L$  and  $H$ —or  $\varepsilon$  and  $\sigma$ —we can plot the flow in different maps that are function of  $g$ ,  $G$ . Figure 1 shows an example in semiequinoctial elements ( $e \cos g, e \sin g$ ), where we note a hyperbolic point corresponding to an unstable circular orbit, and two elliptic points corresponding to two stable elliptic orbits with  $e = 0.2$  and periapsis at  $g = \pm\pi/2$ , respectively.

Delaunay variables are singular for zero eccentricity orbits, where the argument of the periapsis and the mean anomaly are not defined, and for equatorial orbits, where the

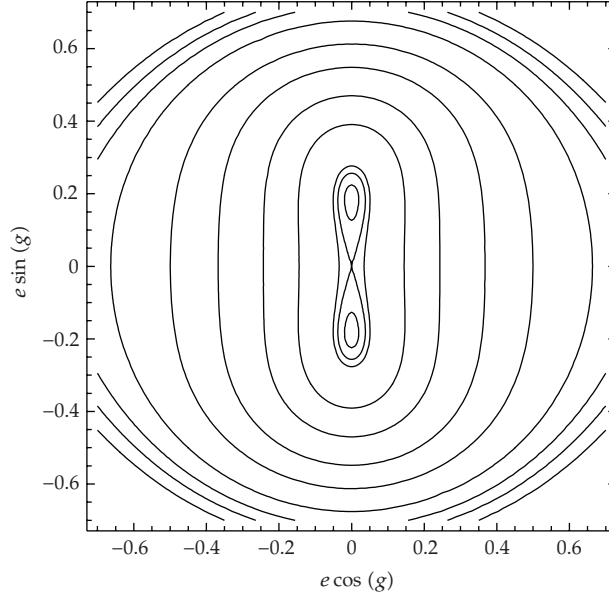


**Figure 1:** Flow in the doubly reduced phase space.

argument of the node is not defined. Hence, it is common to study the reduced phase space in the variables introduced by Coffey et al. [16], see also [8]:

$$\chi_1 = \eta e s \cos g, \quad \chi_2 = \eta e s \sin g, \quad \chi_3 = \eta^2 - \frac{1}{2} (1 + \sigma^2), \quad (3.1)$$

that define the surface of a sphere

$$\chi_1^2 + \chi_2^2 + \chi_3^2 = \frac{1}{4} (1 - \sigma^2)^2 \quad (3.2)$$

of radius  $R = (1/2) (1 - \sigma^2)$  (the sphere representation misses the case  $G = H = 0$ , irrelevant in astrodynamics.)

Then, after dropping constant terms and scaling, Hamiltonian (2.3) writes

$$\begin{aligned} \mathcal{K} = & -12\eta^2 - \frac{30\chi_2^2}{\eta^2} + \frac{9}{4} \varepsilon \sigma \left( 25 - 24\eta^2 - \sigma^2 - 15 \frac{\chi_2^2}{\eta^2} \right) \\ & + \frac{\varepsilon^2}{64} \left[ 3815 + 9528\sigma^2 + 9\sigma^4 - 6 (343 + 1709\sigma^2) \eta^2 - 1824\eta^4 \right. \\ & \left. + 6 (293 - 821\eta^2 - 1470\sigma^2) \frac{\chi_2^2}{\eta^2} - 3285 \frac{\chi_2^4}{\eta^4} \right]. \end{aligned} \quad (3.3)$$

The flow on the sphere is obtained from Liouville equations  $\dot{\chi}_i = \{\chi_i; \mathcal{K}\}$ ,  $i = 1, 2, 3$ , where the dot means derivative in the new time scale. Then,

$$\begin{aligned} \dot{\chi}_1 = \frac{3}{16\eta} \chi_2 \left\{ 64 (5 - 8\eta^2 + 5\sigma^2) + 72\varepsilon\sigma (5 - 2\eta^2 + 5\sigma^2) \right. \\ \left. + \frac{\varepsilon^2}{64} \left[ 3815 - 1824\eta^4 + 9528\sigma^2 + 9\sigma^4 - 6\eta^2(343 + 1709\sigma^2) \right. \right. \\ \left. \left. + 6(293 - 821\eta^2 - 1470\sigma^2) \left( \frac{\chi_2}{\eta} \right)^2 - 3285 \left( \frac{\chi_2}{\eta} \right)^4 \right] \right\}, \end{aligned} \quad (3.4)$$

$$\begin{aligned} \dot{\chi}_2 = -\frac{3}{16\eta} \chi_1 \left\{ 608\varepsilon^2\eta^4 + \eta^2 [128 + 576\varepsilon\sigma + \varepsilon^2 (343 + 1709\sigma^2)] \right. \\ \left. - [320 + 360\varepsilon\sigma - \varepsilon^2(293 - 1470\sigma^2)] \left( \frac{\chi_2}{\eta} \right)^2 - 1095\varepsilon^2 \left( \frac{\chi_2}{\eta} \right)^4 \right\}, \end{aligned} \quad (3.5)$$

$$\dot{\chi}_3 = \frac{3}{8\eta} \chi_1 \chi_2 \left\{ 320 + 360\varepsilon\sigma - \varepsilon^2 \left[ 293 - 1470\sigma^2 - 821\eta^2 - 1095 \left( \frac{\chi_2}{\eta} \right)^2 \right] \right\}, \quad (3.6)$$

with the constraint  $\chi_1 \dot{\chi}_1 + \chi_2 \dot{\chi}_2 + \chi_3 \dot{\chi}_3 = 0$ , derived from (3.2).

Equations (3.4)–(3.6) show that circular orbits ( $\chi_1 = \chi_2 = 0$ ,  $\chi_3 = R$ , the “north” pole of the sphere) are always equilibria. Equations (3.5) and (3.6) vanish when  $\chi_1 = 0$ ,  $\chi_2 \neq 0$ , but (3.4) vanishes only when

$$\begin{aligned} 1095\varepsilon^2\sigma^4 - \sigma^2 [320 + 360\varepsilon\sigma + \varepsilon^2(802 + 2565\sigma^2)] \eta^2 \\ + [192 - 216\varepsilon\sigma - \varepsilon^2(362 - 35\sigma^2)] \eta^6 - 61\varepsilon^2\eta^8 = 0. \end{aligned} \quad (3.7)$$

Equation (3.7) is a polynomial equation of degree 8 in  $\eta$ , therefore admitting eight roots. Note that, for the accepted values of  $\varepsilon \ll 1$ , (3.7) is of the form  $A_1^2 - A_2^2 x + A_3^2 x^3 - A_4^2 x^4 = 0$  that admits a maximum of three real roots, according to Descartes’ rule of signs.

The real roots of (3.7) verified by the dynamical constraint  $|\sigma| \leq \eta \leq 1$  are also equilibria. The root  $\eta = 1$  marks a change in the number of equilibria due to a “bifurcation” ( $\eta > 1$  could be a root but not an equilibrium). Then, the number of equilibria changes when crossing the line

$$\varepsilon = 4 \frac{-27\sigma - 45\sigma^3 \pm \sqrt{5076 + 1473\sigma^2 + 4730\sigma^4 - 27375\sigma^6}}{423 + 767\sigma^2 + 1470\sigma^4} \quad (3.8)$$

obtained setting  $\eta = 1$  in (3.7) that establishes a relation between the dynamical parameters  $\varepsilon$  and  $\sigma$  corresponding to bifurcations of circular orbits. Figure 2 shows that this line defines two regions in the parameters plane with different number of equilibria in phase space. Circular orbits in the outside region of the curve are stable. When crossing the line given by (3.8) the number of real roots of (3.7) with dynamical sense increases such that a pitchfork

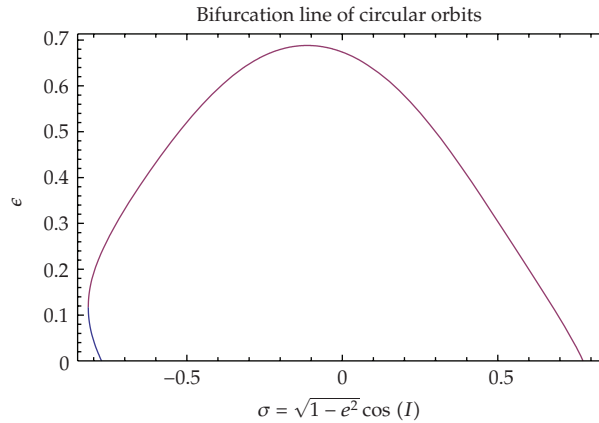


Figure 2: Regions in the parameters plane with different numbers of equilibria.

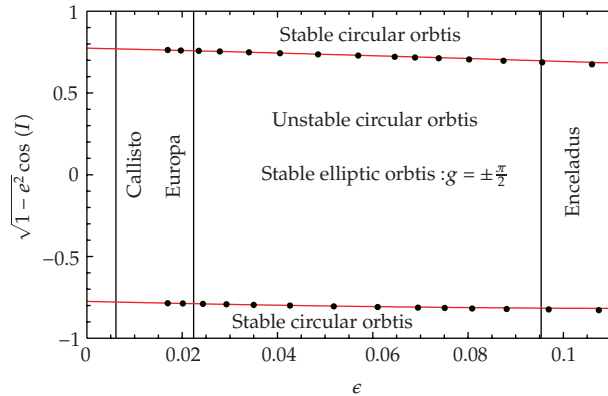
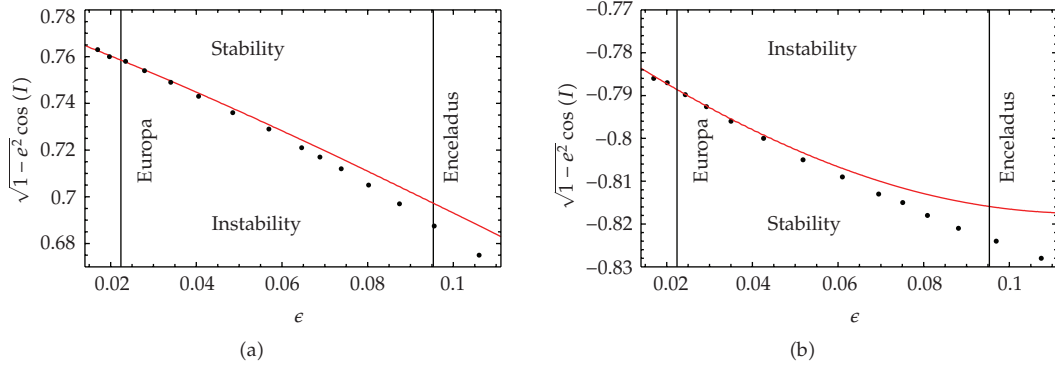


Figure 3: Bifurcation lines in the parameter plane.

bifurcation takes place: circular orbits change to unstable and two stable elliptic orbits appear with periapsis, respectively at  $g = \pm\pi/2$ , as in the example of Figure 1.

Note that the curve given by (3.8) notably modifies the classical inclination limit  $\cos^2 I > 3/5$  for circular orbits' stability. However, we cannot extend the practical application of the analytical theory to any value of  $\epsilon$ . It is common to limit the validity of the Hill problem approximation to one third of the Hill radius  $r_H = 3^{-1/3}$ . Then  $\epsilon < (r_H/3)^{3/2} = 1/9$ , including most of the planetary satellites of interest. Figure 3 shows the bifurcation lines of circular orbits in the validity region of the parameters plane with the values of  $\epsilon$  corresponding to low altitude orbits around different planetary satellites highlighted.

A powerful test for estimating the quality of the analytical theory is to check the degree of agreement of the bifurcation lines of the analytical theory with those computed numerically in the nonaveraged problem. To do that we compute several families of three-dimensional, almost circular, periodic orbits of the Hill (nonaveraged) problem that bifurcate from the family of planar retrograde orbits at different resonances. For variations of the Jacobi constant the almost circular periodic orbits evolve from retrograde to direct orbits through the 180 degrees of inclination. At certain critical points, almost circular orbits change from stable to unstable in a bifurcation phenomenon in which two new elliptic periodic orbits appear.



**Figure 4:** Comparison between the bifurcation line of circular, averaged orbits (full line), and the curve of critical periodic orbits (dots).

**Table 1:** Initial orbital elements of an elliptic frozen orbit for  $\varepsilon = 0.0470573$ ,  $\sigma = 0.422618$ .

Theory	$a$ (Hill units)	$e$	$I$ (deg)	$g$ (deg)	$h$	$\ell$
Classical	0.130342	0.674094	55.0995	-90	0	0
2nd order	0.130342	0.648065	55.6915	-90	0	0
3rd order	0.130515	0.637316	56.1798	-90	0	0
4th order	0.130538	0.634803	56.2813	-90	0	0

The computation of a variety of these critical points helps in determining stability regions for almost circular orbits [17].

The tests done show that the fourth-order theory gives good results for  $\varepsilon < 0.05$ . As presented in Figure 4, the bifurcation line of retrograde orbits clearly diverges from the line of corresponding critical periodic orbits for higher values of  $\varepsilon$ , and it may be worth developing a higher-order theory that encompasses also the case of Enceladus.

## 4. Frozen Orbits Computation

Hill's case of orbits close to the smaller primary is a simplification of the restricted three-body problem, which in turn is a simplification of real models. Therefore, the final goal of our theory is not the generation of ephemerides but to help in mission designing for artificial satellites about planetary satellites, where frozen orbits are of major interest.

For given values of the parameters  $\varepsilon$ ,  $\sigma$ , determined by the mission, a number of frozen orbits may exist. A circular frozen orbit, either stable or unstable, exists always and the computation of real roots  $|\sigma| \leq \eta \leq 1$  of (3.7), if any, will provide the eccentricities of the stable elliptic solutions with frozen periapsis at  $g = \pm\pi/2$ . To each equilibrium of the doubly reduced phase space it corresponds a torus of quasiperiodic solutions in the original, nonaveraged model. In what follows we present several examples that justify the effort in computing a fourth-order theory to reach the quasiperiodicity condition in the Hill problem.

### 4.1. Elliptic Frozen Orbits

We choose  $\varepsilon = 0.0470573$ ,  $\sigma = 0.422618$ . If we first try the classical double-averaged solution, the Hamiltonian (2.3) is simplified to  $K_{0,0} + \varepsilon K_{0,1} + (\varepsilon^2/2)K_{0,2}$ , and the existence of elliptic



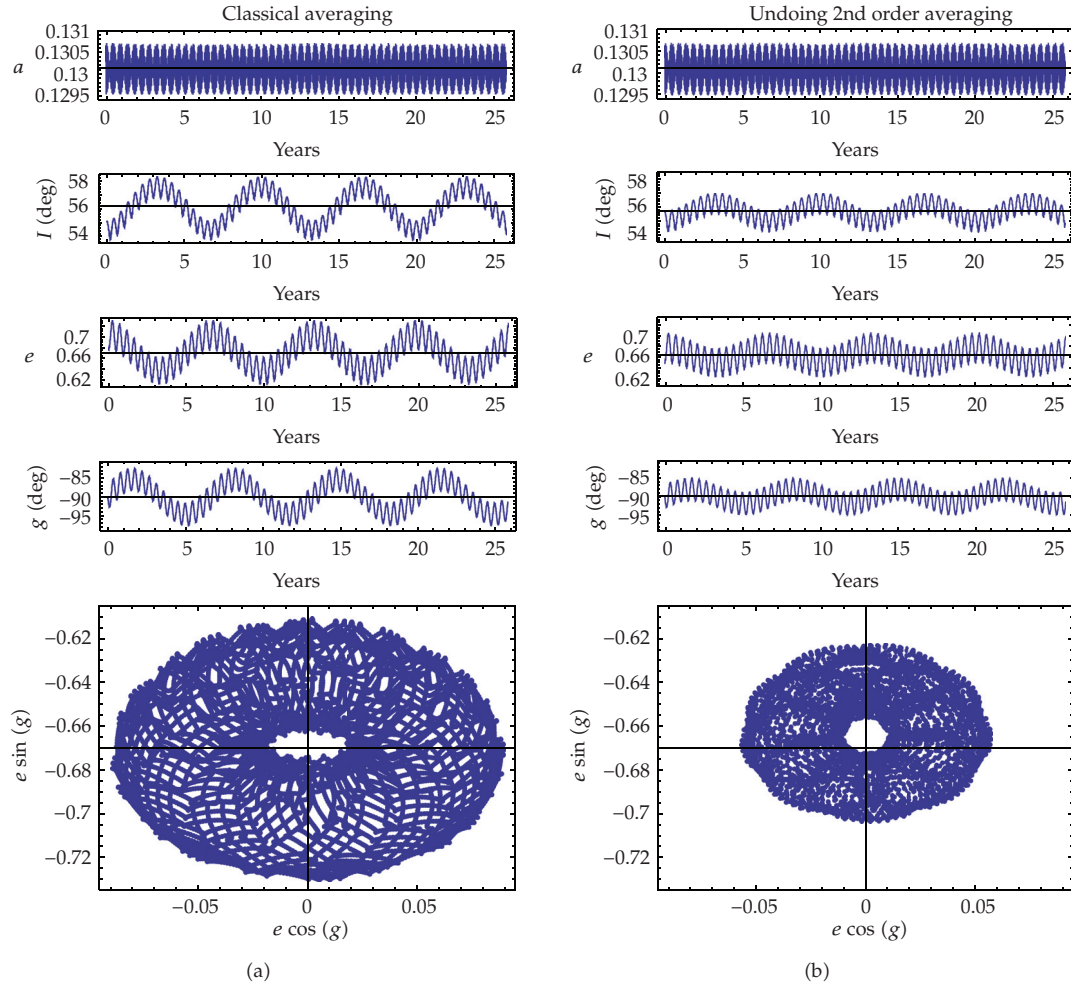


Figure 5: Long-term evolution of the orbital elements of the elliptic frozen orbit.

frozen orbits reduces to the case  $\sigma^2 < 3/5$ ,  $g = \pm\pi/2$ . The eccentricity of the elliptic frozen solutions is then computed from  $\eta = (5\sigma^2/3)^{1/4}$ —obtained by neglecting terms in  $\varepsilon$  in (3.7). Thus, for the given values of  $\varepsilon$  and  $\sigma$ , and taking into account that we are free to choose the initial values of the averaged angles  $\ell$ ,  $h$ , we get the orbital elements of the first row of Table 1. The left column of Figure 5 shows the long-term evolution of the instantaneous orbital elements for this case, that we call “classical averaging,” in which we find long-period oscillations of more than four degrees in inclination, more than fifteen in the argument of periastris, and a variation of  $\pm 0.06$  in the eccentricity.

When computing a second-order theory with the Lie-Deprit perturbation method we arrive exactly at the classical Hamiltonian obtained by a simple removal of the short-period terms and the classical bifurcation condition that results in the critical inclination of the third-body perturbations  $I = 39.2^\circ$  [10, 11]. However, now we have available the transformation equations to recover the short- and long-period effects, although up to the first order only. After undoing the transformation equations we find the orbital elements of the second row of Table 1, where we see that all the elements remain unchanged except for

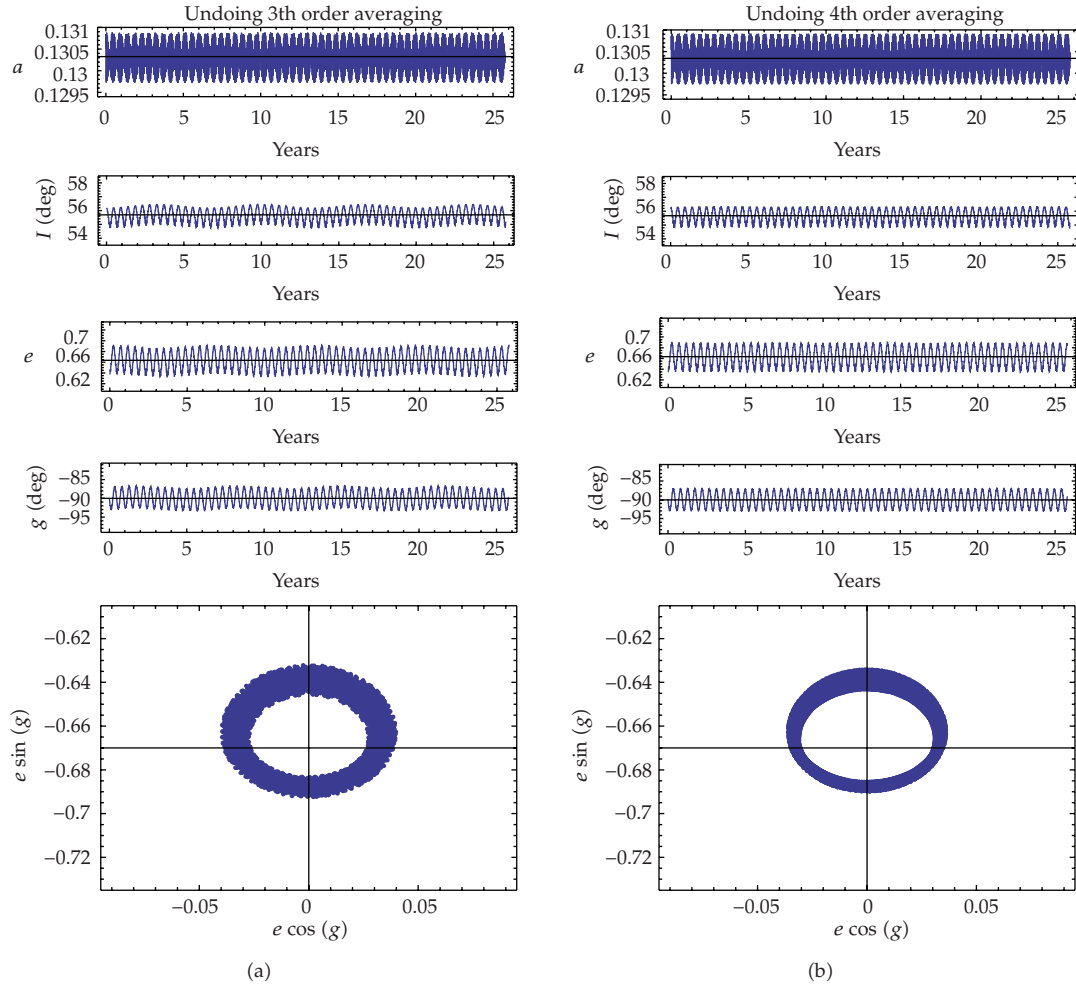


Figure 6: Long-term evolution of the orbital elements of the elliptic frozen orbit.

the eccentricity and inclination. The long-term evolution of these elements is presented in the right column of Figure 5, in which we notice a significant reduction in the amplitude of long-period oscillations:  $2.5^\circ$  in inclination, around  $10^\circ$  in the argument of the periapsis, and  $\pm 0.04$  in eccentricity.

The results of the third- and fourth-order theories are presented in the last two rows of Table 1 and in Figure 6. The higher-order corrections drive slight enlargements in the semimajor axis. While both higher-order theories produce impressive improvements, we note a residual long-period oscillation in the elements computed from the third-order theory (left column of Figure 6). On the contrary, the orbital elements of the frozen orbit computed with the fourth-order theory are almost free from long-period oscillations and mainly show the short-period oscillations typical of quasiperiodic orbits.

#### 4.2. Circular Frozen Orbits

If we choose the same value for  $\varepsilon$  but now  $\sigma = 0.777146$ , frozen elliptic orbits do not exist any longer and the circular frozen orbit is stable. Both the third and fourth-order theories provide

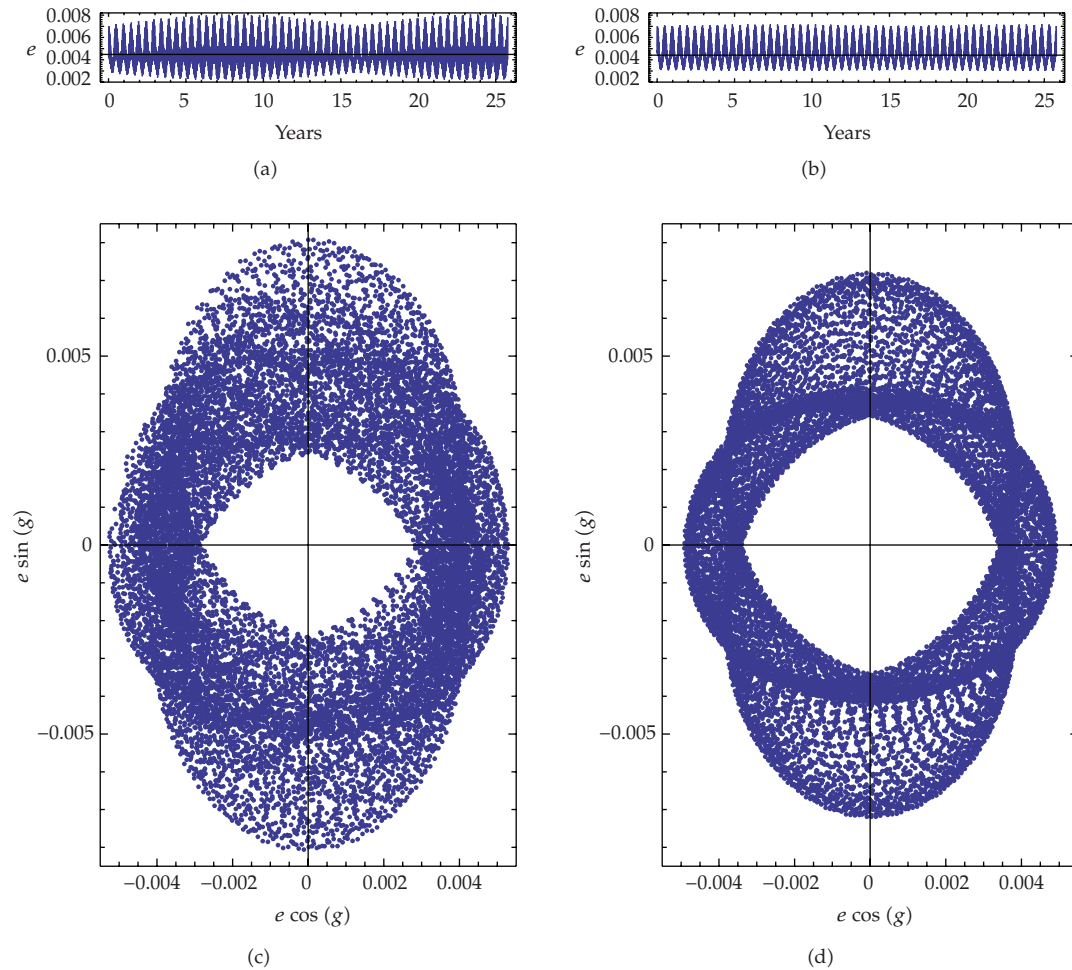


**Figure 7:** Long-term evolution of the orbital elements of the circular stable frozen orbit. (a) and (c) third-order theory. (b) and (d) fourth-order theory.

good results, but, again, the third-order theory provides small long-period oscillations in the eccentricity whereas the fourth-order theory leads to a quasiperiodic orbit (see Figure 7).

For  $\varepsilon = 0.0339919$  and  $\sigma = 0.34202$  the circular frozen orbit is unstable. Due to the instability, a long-term propagation of the initial conditions from either the third or the fourth theory shows that the orbit escapes following the unstable manifold with exponential increase in the eccentricity. But, as Figure 8 shows, the orbit remains frozen much more time when using the fourth-order theory. A variety of tests performed on science orbits close to Galilean moons Europa and Callisto showed that the fourth-order theory generally improves by 50% the lifetimes reached when using the third-order theory.

### 4.3. Fourier Analysis

Alternatively to the temporal analysis mentioned previously, a frequency analysis using the Fast Fourier Transform (FFT) shows how initial conditions obtained from different orders of the analytical theory can be affected of undesired frequencies that defrost the orbital elements.

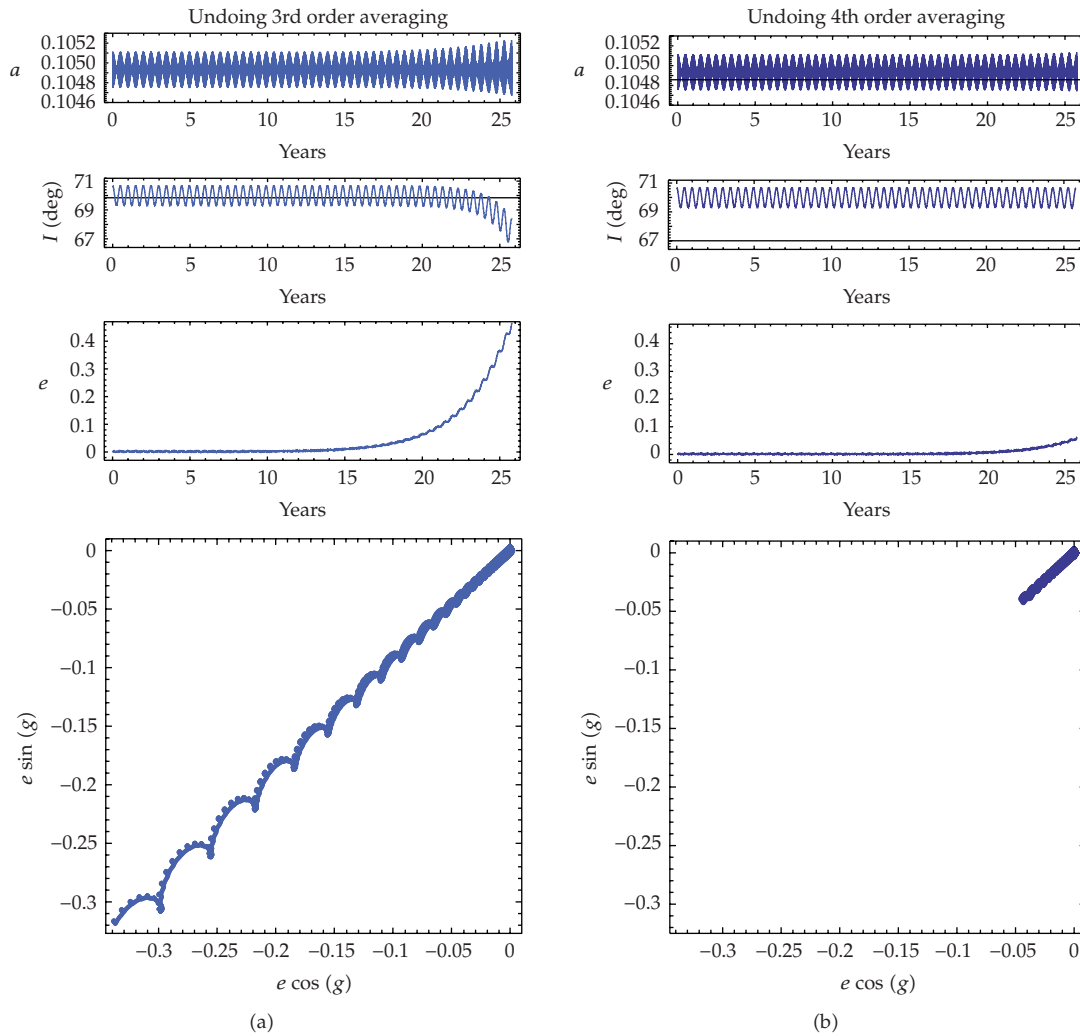


**Figure 8:** Long-term evolution of the orbital elements of the circular, unstable, frozen orbit.

Thus, Figure 9 shows the FFT analysis of the instantaneous argument of the periapsis of the elliptic orbit in the example mentioned previously. Dots correspond to initial conditions obtained from the double-averaged phase space after a classical analysis—that is equivalent to the second-order analytical theory—and the line corresponds to initial conditions obtained from the fourth-order analytical theory after undoing the transformation. While most of the frequencies match with similar amplitudes, in the magnification of the right plot we clearly appreciate a very low frequency of  $\sim 0.15$  cycles/year with a very high amplitude in the classical theory that is almost canceled out with the fourth-order approach. The semiannual frequency remains in both theories because it is intrinsic to the problem. It is due to the third-body perturbation and it cannot be avoided.

Figure 10 shows a similar analysis for the instantaneous eccentricity of the stable circular orbit mentioned previously. Now, dots correspond to the fourth-order theory and the line to the third-order one (both after undoing the transformation equations). While the

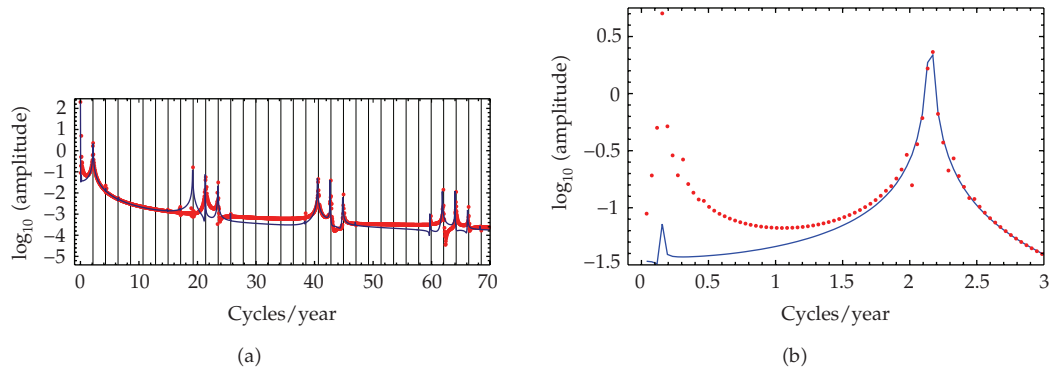


**Figure 9:** (a) FFT analysis of the instantaneous argument of the periaapsis of the elliptic solution. (b) Magnification over the low frequencies region.

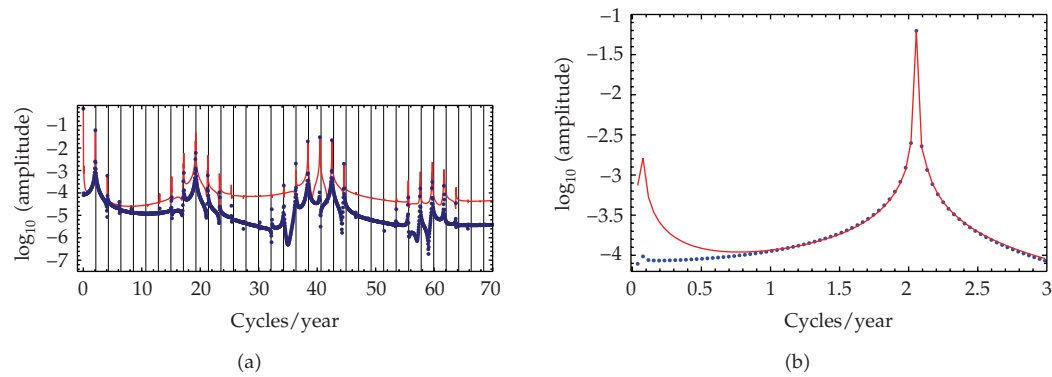


**Figure 10:** (a) FFT analysis of the instantaneous eccentricity of the elliptic solution. (b) Magnification over the low frequencies region.

third-order theory provides good results, reducing the amplitude of the undesired frequency to low values, the fourth-order theory practically cancels out that frequency.

An FFT analysis of unstable circular orbits has not much sense because of the time scale in which the orbit destabilizes.

## 5. Conclusions

Frozen orbits computation is a useful procedure in mission designing for artificial satellites. After locating the frozen orbit of interest in a double-averaged problem, usual procedures for computing initial conditions of frozen orbits resort to trial-and-error interactive corrections, or require involved computations. However, the explicit transformation equations between averaged and nonaveraged models can be obtained with analytical theories based on the Lie-Deprit perturbation method, which makes the frozen orbits computations straightforward.

Accurate computations of the initial conditions of frozen, quasiperiodic orbits can be reached with higher-order analytical theories. This way of proceeding should not be undervalued in the computation of science orbits around planetary satellites, a case in which third-body perturbations induce unstable dynamics.

Higher-order analytical theories are a common tool for computing ephemeris among the celestial mechanics community. They are usually developed with specific purpose, sophisticated algebraic manipulators. However, the impressive performances of modern computers and software allow us to build our analytical theory with commercial, general-purpose manipulators, a fact that may challenge aerospace engineers to use the safe, well-known techniques advocated in this paper.

## Appendix

Let  $\mathcal{T} : (\mathbf{x}, \mathbf{X}) \rightarrow (\mathbf{x}', \mathbf{X}')$ , where  $\mathbf{x}$  are coordinates and  $\mathbf{X}$  their conjugate momenta, be a Lie transform from “new” (primes) to “old” variables. If  $W = \sum_i (\epsilon^i / i!) W_{i+1}(\mathbf{x}, \mathbf{X})$  is its generating function expanded as a power series in a small parameter  $\epsilon$ , a function  $\mathcal{F} = \sum_i (\epsilon^i / i!) F_{i,0}(\mathbf{x}, \mathbf{X})$  can be expressed in the new variables as the power series  $(\mathcal{T} : \mathcal{F}) = \sum_i (\epsilon^i / i!) F_{0,i}(\mathbf{x}', \mathbf{X}')$  whose coefficients are computed from the recurrence

$$F_{i,j} = F_{i+1,j-1} + \sum_{0 \leq k \leq i} \binom{i}{k} \{F_{k,j-1}; W_{i+1-k}\}, \quad (\text{A.1})$$

where  $\{F_{k,j-1}; W_{i+1-k}\} = \nabla_{\mathbf{x}} F_{k,j-1} \cdot \nabla_{\mathbf{X}} W_{i+1-k} - \nabla_{\mathbf{X}} F_{k,j-1} \cdot \nabla_{\mathbf{x}} W_{i+1-k}$ , is the Poisson bracket. Conversely, the coefficients  $W_{i+1}$  of the generating function can be computed step by step from (A.1) once corresponding terms  $F_{0,i}$  of the transformed function are chosen as desired. In perturbation theory it is common to chose the  $F_{0,i}$  as an averaged expression over some variable, but it is not the unique possibility [18]. Full details can be found in the literature [19, 20].

To average the short-period effects we write Hamiltonian (2.2) in Delaunay variables as

$$\mathcal{H} = H_{0,0} + \epsilon H_{1,0} + \left(\frac{\epsilon^2}{2}\right) H_{2,0} + \left(\frac{\epsilon^3}{6}\right) H_{3,0} + \left(\frac{\epsilon^4}{24}\right) H_{4,0}, \quad (\text{A.2})$$

where  $H_{0,0} = -1/(2L^2)$ ,  $H_{1,0} = -H$ ,  $H_{2,0} = r^2 \{1 - 3[\cos(f+g)\cos h - c \sin(f+g)\sin h]^2\}$ , and  $H_{3,0} = H_{4,0} = 0$ . Note that the true anomaly  $f$  is an implicit function of  $\ell$ .

Since the radius  $r$  never appears in denominators, it results convenient to express Hamiltonian (A.2) as a function of the elliptic—instead of the true—anomaly  $u$  by using the ellipse relations  $r \sin f = \eta a \sin u$ ,  $r \cos f = a(\cos u - e)$ ,  $r = a(1 - e \cos u)$ .

After applying the Delaunay normalization [21] up to the fourth-order in the Hamiltonian, we get

$$\mathcal{H}' = H_{0,0} + \epsilon H_{0,1} + \left(\frac{\epsilon^2}{2}\right) H_{0,2} + \left(\frac{\epsilon^3}{6}\right) H_{0,3} + \left(\frac{\epsilon^4}{24}\right) H_{0,4}, \quad (\text{A.3})$$

where, omitting primes,

$$H_{0,0} = -\frac{1}{2L^2},$$

$$H_{0,1} = H_{0,0} \epsilon 2c \eta,$$

$$\begin{aligned}
H_{0,2} &= H_{0,0} \left( \frac{\varepsilon^2}{8} \right) \left\{ (4 + 6e^2) (2 - 3s^2 + 3s^2 \cos 2h) \right. \\
&\quad \left. + 15e^2 [2s^2 \cos 2g + (1 - c)^2 \cos(2g - 2h) + (1 + c)^2 \cos(2g + 2h)] \right\}, \\
H_{0,3} &= H_{0,0} \left( \frac{45\varepsilon^3}{8} \right) e^2 \eta \left[ (1 + c)^2 \cos(2g + 2h) - (1 - c)^2 \cos(2g - 2h) \right], \\
H_{0,4} &= H_{0,0} \left( -\frac{3\varepsilon^4}{512} \right) \\
&\quad \times \left\{ 16(47 + 282c^2 + 63c^4) - 144(227 + 90c^2 + 59c^4) e^2 \right. \\
&\quad - 18(227 + 610c^2 - 701c^4) e^4 - 24s^2 [558 + 270c^2 + (109 - 555c^2) e^2] e^2 \cos 2g \\
&\quad + 24s^2 [216 + 56c^2 - 8(161 + 59c^2) e^2 - (11 - 701c^2) e^4] \cos 2h \\
&\quad - 48(1 + c)^2 [338 - 90c + 90c^2 - (91 - 185c + 185c^2) e^2] e^2 \cos(2g + 2h) \\
&\quad - 48(1 - c)^2 [338 + 90c + 90c^2 - (91 + 185c + 185c^2) e^2] e^2 \cos(2g - 2h) \\
&\quad + 6s^4 (56 - 472e^2 + 701e^4) \cos 4h + 1710s^4 e^4 \cos 4g \\
&\quad - 60s^2 (18 - 37e^2) e^2 [(1 + c)^2 \cos(2g + 4h) + (1 - c)^2 \cos(2g - 4h)] \\
&\quad + 1140s^2 e^4 [(1 + c)^2 \cos(4g + 2h) + (1 - c)^2 \cos(4g - 2h)] \\
&\quad \left. + 285e^4 [(1 + c)^4 \cos(4g + 4h) + (1 - c)^4 \cos(4g - 4h)] \right\}.
\end{aligned} \tag{A.4}$$

The generating function of the transformation is  $W = W_2 + (1/2)W_3$ , where

$$\begin{aligned}
W_2 &= L \left( \frac{\varepsilon^2}{192} \right) \\
&\quad \times \left\{ 4(2 - 3s^2) [3e(5 + 3\eta^2) S_{1,0,0} - 9e^2 S_{2,0,0} + e^3 S_{3,0,0}] \right. \\
&\quad + 6s^2 e [3(5 + 3\eta^2) (S_{1,0,2} + S_{1,0,-2}) - 9e(S_{2,0,2} + S_{2,0,-2}) + e^2(S_{3,0,2} + S_{3,0,-2})] \\
&\quad + 6s^2 (1 + \eta)^2 [15e S_{1,2,0} - (9 - 6\eta) S_{2,2,0} + e S_{3,2,0}] \\
&\quad + 6s^2 (1 - \eta)^2 [15e S_{1,-2,0} - (9 + 6\eta) S_{2,-2,0} + e S_{3,-2,0}] \\
&\quad \left. + 3(1 + c)^2 (1 + \eta)^2 [15e S_{1,2,2} - (9 - 6\eta) S_{2,2,2} + e S_{3,2,2}] \right\}
\end{aligned}$$

$$\begin{aligned}
& + 3(1-c)^2(1+\eta)^2 [15eS_{1,2,-2} - (9-6\eta)S_{2,2,-2} + eS_{3,2,-2}] \\
& + 3(1-c)^2(1-\eta)^2 [15eS_{1,-2,2} - (9+6\eta)S_{2,-2,2} + eS_{3,-2,2}] \\
& + 3(1+c)^2(1-\eta)^2 [15eS_{1,-2,-2} - (9+6\eta)S_{2,-2,-2} + eS_{3,-2,-2}] \}, \\
W_3 = L \left( \frac{\varepsilon^3}{256} \right) \\
& \times \left\{ 72e^2 s^2 (13 + 3\eta^2) [S_{1,0,2} - S_{1,0,-2}] - 24e^2 s^2 (17 + 4\eta^2) [S_{2,0,2} - S_{2,0,-2}] \right. \\
& + 88e^3 s^2 [S_{3,0,2} - S_{3,0,-2}] - 6e^4 s^2 [S_{4,0,2} - S_{4,0,-2}] \\
& + 36e(1+\eta)(13+\eta+8\eta^2) [(1+c)^2 S_{1,2,2} - (1-c)^2 S_{1,2,-2}] \\
& + 36e(1-\eta)(13-\eta+8\eta^2) [(1-c)^2 S_{1,-2,2} - (1+c)^2 S_{1,-2,-2}] \\
& - 12(1+\eta)^2 (17-6\eta-8\eta^2) [(1+c)^2 S_{2,2,2} - (1-c)^2 S_{2,2,-2}] \\
& - 12(1-\eta)^2 (17+6\eta-8\eta^2) [(1-c)^2 S_{2,-2,2} - (1+c)^2 S_{2,-2,-2}] \\
& + 4(1+\eta)^2 e(11-6\eta) [(1+c)^2 S_{3,2,2} - (1-c)^2 S_{3,2,-2}] \\
& + 4(1-\eta)^2 e(11+6\eta) [(1-c)^2 S_{3,-2,2} - (1+c)^2 S_{3,-2,-2}] \\
& - 3(1+\eta)^2 e^2 [(1+c)^2 S_{4,2,2} - (1-c)^2 S_{4,2,-2}] \\
& \left. - 3(1-\eta)^2 e^2 [(1-c)^2 S_{4,-2,2} - (1+c)^2 S_{4,-2,-2}] \right\}. \tag{A.5}
\end{aligned}$$

We shorten notation calling  $S_{i,j,k} \equiv \sin(i u + j g + k h)$ .

The Lie transform of generating function  $W$  can be applied to any function of Delaunay variables  $\mathcal{F} = \sum_i (\varepsilon^i / i!) F_i(\ell', g', h', L', G', H')$ . Since  $W_1 = 0$ , up to the third-order in the small parameter recurrence (A.1) gives

$$\mathcal{F} = F_0 + \left( \frac{\varepsilon^2}{2} \right) \{F_0; W_2\} + \left( \frac{\varepsilon^3}{6} \right) \{F_0; W_3\}. \tag{A.6}$$

Specifically, this applies to the transformation equations of the Delaunay variables themselves, where  $F_0 \in (\ell', g', h', L', G', H')$  and  $F_i \equiv 0$  for  $i > 0$ .

A new application of the recurrence (A.1) to the Hamiltonian  $\mathcal{K} = \sum_{0 \leq i \leq 4} (\varepsilon^i / i!) K_{i,0}$ , where  $K_{i,0} \equiv H_{0,i}$  of (A.3), allows to eliminate the node up to the fourth-order, obtaining the double-averaged Hamiltonian (2.3). Note that  $K_{0,4}$  corrects previous results in [22]. The generating function of the transformation is  $V = V_1 + \varepsilon V_2 + (\varepsilon^2 / 2) V_3$ , where, omitting double



primes,

$$\begin{aligned}
V_1 &= L\left(\frac{3}{64}\right)\left[\left(4+6e^2\right)s^2\sin 2h+5(1+c)^2e^2\sin(2g+2h)-5(1-c)^2e^2\sin(2g-2h)\right], \\
V_2 &= L\left(-\frac{3}{128}\right)\eta\left[6c\left(2-17e^2\right)s^2\sin 2h+5(2-9c)(1+c)^2e^2\sin(2g+2h)\right. \\
&\quad \left.+5(1-c)^2(2+9c)e^2\sin(2g-2h)\right], \\
V_3 &= L\left(-\frac{9}{32768}\right) \\
&\quad \times\left\{16s^2\left[456-104c^2-8(193+754c^2)e^2+(47+7831c^2)e^4\right]\sin 2h\right. \\
&\quad +2s^4\left(232+416e^2-1803e^4\right)\sin 4h \\
&\quad -32(1+c)^2e^2\left[2(323-285c+780c^2)-(527-1135c+2125c^2)e^2\right]\sin(2g+2h) \\
&\quad +32(1-c)^2e^2\left[2(323+285c+780c^2)-(527+1135c+2125c^2)e^2\right]\sin(2g-2h) \\
&\quad +220s^2e^2(4-11e^2)\left[(1+c)^2\sin(2g+4h)-(1-c)^2\sin(2g-4h)\right] \\
&\quad +4520s^2e^4\left[(1+c)^2\sin(4g+2h)-(1-c)^2\sin(4g-2h)\right] \\
&\quad \left.-385e^4\left[(1+c)^4\sin(4g+4h)-(1-c)^4\sin(4g-4h)\right]\right\}. \tag{A.7}
\end{aligned}$$

The new Lie transform of generating function  $V$  can be applied to any function of Delaunay variables, and, specifically, to the Delaunay variables themselves. For any  $\xi'' \in (\ell'', g'', h'', L'', G'', H'')$  the transformation equations of the Lie transform are computed, up to the third-order, from

$$\xi' = \xi'' + \varepsilon\delta_1 + \left(\frac{\varepsilon^2}{2}\right)\delta_2 + \left(\frac{\varepsilon^3}{6}\right)\delta_3, \tag{A.8}$$

where

$$\begin{aligned}
\delta_1 &= \{\xi''; V_1\}, \\
\delta_2 &= \{\xi''; V_2\} + \{\delta_1; V_1\}, \\
\delta_3 &= \{\xi''; V_3\} + \{\{\xi''; V_2\}; V_1\} + \{\delta_1; V_2\} + \{\delta_2; V_1\}.
\end{aligned} \tag{A.9}$$

## Acknowledgments

This work was supported from Projects ESP 2007-64068 (the first author) and MTM 2008-03818 (the second author) of the Ministry of Science and Innovation of Spain is

acknowledged. Part of this work has been presented at 20th International Symposium on Space Flight Dynamics, Annapolis, Maryland, USA, September, 24–28 2007.

## References

- [1] G. W. Hill, "Researches in the lunar theory," *American Journal of Mathematics*, vol. 1, no. 2, pp. 129–147, 1878.
- [2] M. L. Lidov, "The evolution of orbits of artificial satellites of planets under the action of gravitational perturbations of external bodies," *Planetary and Space Science*, vol. 9, no. 10, pp. 719–759, 1962, translated from *Iskusstvennye Sputniki Zemli*, no. 8, p. 5, 1961.
- [3] M. Hénon, "Numerical exploration of the restricted problem. VI. Hill's case: non-periodic orbits," *Astronomy and Astrophysics*, vol. 9, pp. 24–36, 1970.
- [4] D. P. Hamilton and A. V. Krivov, "Dynamics of distant moons of asteroids," *Icarus*, vol. 128, no. 1, pp. 241–249, 1997.
- [5] Y. Kozai, "Motion of a lunar orbiter," *Publications of the Astronomical Society of Japan*, vol. 15, no. 3, pp. 301–312, 1963.
- [6] M. L. Lidov and M. V. Yarskaya, "Integrable cases in the problem of the evolution of a satellite orbit under the joint effect of an outside body and of the noncentrality of the planetary field," *Kosmicheskii Issledovaniya*, vol. 12, pp. 155–170, 1974.
- [7] D. J. Scheeres, M. D. Guman, and B. F. Villac, "Stability analysis of planetary satellite orbiters: application to the Europa orbiter," *Journal of Guidance, Control and Dynamics*, vol. 24, no. 4, pp. 778–787, 2001.
- [8] M. Lara, J. F. San-Juan, and S. Ferrer, "Secular motion around synchronously orbiting planetary satellites," *Chaos*, vol. 15, no. 4, pp. 1–13, 2005.
- [9] M. E. Paskowitz and D. J. Scheeres, "Orbit mechanics about planetary satellites including higher order gravity fields," in *Proceedings of the Space Flight Mechanics Meeting*, Copper Mountain, Colo, USA, January 2005.
- [10] Y. Kozai, "Secular perturbations of asteroids with high inclination and eccentricity," *The Astronomical Journal*, vol. 67, no. 9, pp. 591–598, 1962.
- [11] R. A. Broucke, "Long-term third-body effects via double averaging," *Journal of Guidance, Control and Dynamics*, vol. 26, no. 1, pp. 27–32, 2003.
- [12] M. E. Paskowitz and D. J. Scheeres, "Design of science orbits about planetary satellites: application to Europa," *Journal of Guidance, Control and Dynamics*, vol. 29, no. 5, pp. 1147–1158, 2006.
- [13] A. Deprit, "Canonical transformations depending on a small parameter," *Celestial Mechanics*, vol. 1, no. 1, pp. 12–30, 1969.
- [14] M. Lara, "Simplified equations for computing science orbits around planetary satellites," *Journal of Guidance, Control, and Dynamics*, vol. 31, no. 1, pp. 172–181, 2008.
- [15] A. Deprit and A. Rom, "The main problem of artificial satellite theory for small and moderate eccentricities," *Celestial Mechanics*, vol. 2, no. 2, pp. 166–206, 1970.
- [16] S. Coffey, A. Deprit, and E. Deprit, "Frozen orbits for satellites close to an Earth-like planet," *Celestial Mechanis and Dynamical Astronomy*, vol. 59, no. 1, pp. 37–72, 1994.
- [17] M. Lara and D. Scheeres, "Stability bounds for three-dimensional motion close to asteroids," *Journal of the Astronautical Sciences*, vol. 50, no. 4, pp. 389–409, 2002.
- [18] A. Deprit, "The elimination of the parallax in satellite theory," *Celestial Mechanics*, vol. 24, no. 2, pp. 111–153, 1981.
- [19] S. Ferrer and C. A. Williams, "Simplifications toward integrability of perturbed Keplerian systems," *Annals of the New York Academy of Sciences*, vol. 536, pp. 127–139, 1988.
- [20] J. F. Palacián, "Dynamics of a satellite orbiting a planet with an inhomogeneous gravitational field," *Celestial Mechanis and Dynamical Astronomy*, vol. 98, no. 4, pp. 219–249, 2007.
- [21] A. Deprit, "Delaunay normalisations," *Celestial Mechanics*, vol. 26, no. 1, pp. 9–21, 1982.
- [22] J. F. San-Juan and M. Lara, "Normalizaciones de orden alto en el problema de Hill," *Monografías de la Real Academia de Ciencias de Zaragoza*, vol. 28, pp. 23–32, 2006.